EurJIC European Journal of Inorganic Chemistry
ChemPubSoc Europe
FULL PAPER

DOI:10.1002/ejic.201201413

Rhenium Complexes with a Pyridinyl-Naphthyridine Ligand: Synthesis, Characterization, and Catalytic Activity

Tzu-Chieh Su,[a] Yi-Hung Liu,[a] Shie-Ming Peng,[a] and Shiuh-Tzung Liu*[a]

Keywords: Rhenium / N ligands / Homogenous catalysis / C–H activation

Treatment of $[Re_2(CO)_8(CH_3CN)_2]$ with 2,7-dipyridinyl-1,8-naphthyridine (bpnp) thermally provided mononuclear [(*N*,*N*′-bpnp)$Re(CO)_3Cl$] (**1**). Further reaction of **1** with rhenium carbonyls yielded *ortho*-metallation dinuclear rhenium complex **2**. Both complexes were characterized by spectroscopic analyses and single-crystal X-ray determination. Complex **1** also reacted with [PdMeCl(COD)] and [Ir(COD)Cl]$_2$ by means of *ortho*-metallation to yield the corresponding heterodinuclear species. Complex **2** appears to be an excellent precatalyst to promote the insertion of terminal alkynes into acetoacetates, which subsequently undergo cyclization to form 2-pyranones.

Introduction

Ligands that can accommodate two metal ions in close proximity have received considerable attention in recent years. Such dinuclear complexes may display unusual properties between the metal ions, which are expected to lead to synergic effects particularly in the catalytic reactions.[1] One of the promising dinucleating ligands is 2,7-bis(2-pyridyl)-1,8-naphthyridine (bpnp) (Scheme 1), which was first synthesized by Caluwe in 1979.[2] The distance between two pyridinyl nitrogen donors is about 8.6 Å, which is suitable for constructing a stable dinuclear complex through the chelation of the 1,8-naphthyridine unit. Indeed, this tetradentate has been shown to form stable dinuclear complexes of rhodium,[3] ruthenium,[4] copper,[5] and palladium.[6]

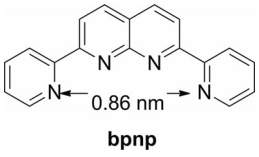

bpnp

Scheme 1. Structure of bpnp.

Kaska and coworkers reported that complexation of bpnp with $[Re(CO)_3Br(THF)_2]$ yielded a mononuclear rhenium complex, [(bpnp)$Re(CO)_3Br$].[7] However, no dinuclear rhenium complex that contains bpnp has been reported. In the present work, we describe the complexes, including mono- and dirhenium species, that were obtained by treating bpnp with rhenium carbonyls. Furthermore, the preparation of the dimetallic Re/Ir and Re/Pd complexes was investigated. The new dirhenium complexes are good catalysts for the insertion of alkynes into β-keto esters.

Results and Discussion

Synthesis and Characterization of Rhenium Complexes

Tetradentate bpnp was prepared according to the reported method.[8] Thermal reaction of $[Re_2(CO)_8(CH_3CN)_2]$ with bpnp in a 1:1 molar ratio in a sealed tube with chlorobenzene as the solvent generated a mixture of air-stable mono- and dirhenium complexes in 100% yield (based on the ligand) (Scheme 2). Both **1** and **2** were isolated in a ratio of 38:62 by a chromatographic separation. By varying the reaction temperature and molar ratio of the reactants, the yield of **2** did not improve significantly. It was noted that the solvents used for the reaction affected the product formation dramatically. If the reaction was carried out in a non-chlorinated organic solvent, such as toluene or xylene, no desired product was obtained. Presumably, this is due to the chloride ligand coming from the solvent

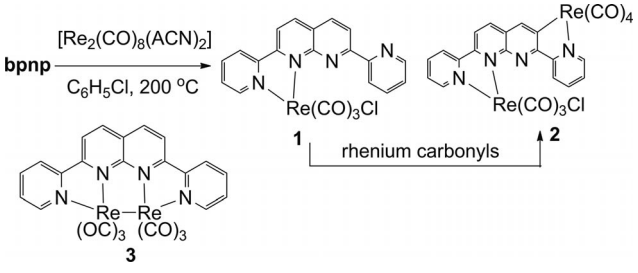

Scheme 2. Preparation of rhenium complexes.

[a] Department of Chemistry, National Taiwan University, 1, Sec. 4, Roosevelt Road, Taipei, Taiwan 106
Fax: +88-62-33668671
E-mail: stliu@ntu.edu.tw
Homepage address: http://www.ch.ntu.edu.tw/

molecule. Complex **1** can be obtained exclusively by the substitution of $[Re(CO)_5Cl]$ with bpnp directly. Treatment of **1** with rhenium carbonyls, such as $[Re_2(CO)_{10}]$ or $[Re_2(CO)_8(CH_3CN)_2]$, provided **2**, but accompanied by various unidentified complexes. However, we did not observe the formation of the expected dirhenium complex **3** in all of the cases, which was presumably due to steric hindrance.[7]

Both **1** and **2** were isolated as crystalline solids and were thoroughly characterized by spectroscopic and X-ray crystallographic analyses. The presence of three CO bands (2015, 1908, and 1884 cm^{-1}) in the IR spectrum of **1** are consistent with the existence of a $Re(CO)_3$ fragment, which is similar to the bromo analog, $[(bpnp)Re(CO)_3Br]$.[7] Although NMR spectroscopic and mass spectroscopic data provided the structural information of **1**, the detailed coordination configurations were confirmed by single-crystal X-ray diffraction analysis of **1**·(H_2O). The ORTEP plot is shown in Figure 1, while some relevant structural parameters are collected in Table 1.

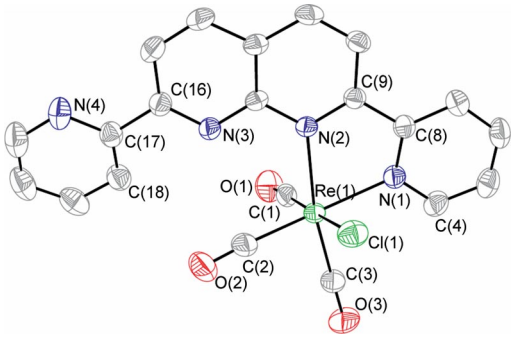

Figure 1. ORTEP plot of **1** (drawn with 30% probability ellipsoids).

Table 1. Selected bond lengths [Å] and angles [°] for **1**.

Bond length		Bond angles	
Re(1)–C(1)	1.907(3)	N(1)–Re(1)–N(2)	74.24(7)
Re(1)–C(2)	1.925(3)	N(1)–Re(1)–Cl(1)	81.82(6)
Re(1)–C(3)	1.899(3)	N(1)–Re(1)–C(1)	99.2(1)
Re(1)–N(1)	2.167(2)	N(1)–Re(1)–C(2)	170.7(1)
Re(1)–N(2)	2.197(2)	N(1)–Re(1)–C(3)	96.6(1)
Re(1)–Cl(1)	2.4956(7)	N(2)–Re(1)–C(3)	170.82(9)

The bipyridine fragment of bpnp and the chloride ligand around the metal center in complex **1** are arranged in a *facial* configuration. This coordination mode is similar to that of $[(bpnp)Re(CO)_3Br]$.[7] Complex **1** adopts a slightly distorted octahedral geometry around the rhenium atom, where the two nitrogen donors constitute a five-member ring with the metal atom. The resulting bite angle is 74.23(7)°. The bond lengths of Re–N in this complex are 2.167(2) and 2.197(2) Å, respectively, whereas the distance of Re–Cl is 2.4957(7) Å. These values compare well to those observed in the related complex, $[(bipyridine)Re(CO)_3Cl]$.[9] The nonplanarity of the naphthyridine core of the uncoordinated bipyridine is observed as evidenced by the dihedral angle of N(3)–C(16)–C(17)–C(18) [12.7(4)°].

The FAB-mass spectrum of **2** shows a molecular ion ($C_{25}H_{11}ClN_4O_7Re_2$) at m/z = 887.9437, which indicates that it is a dirhenium species. The structure of **2** was established by its distinct ^1H NMR spectrum and X-ray crystallography. Utilization of the spin-spin coupling of the adjacent protons allowed for a convenient analysis of the C–H activation in the structure of **2** (Figure 2). Complex **1** displays four sets of doublets for the naphthyridine protons. On the other hand, three sets of signals [two sets of doublets (C5′–*H* and C6′–*H*) and a singlet (C7′–*H*)] appear for the naphthyridine protons in complex **2**, an indication that *ortho*-metallation takes place at the C8′ position. This formulation was confirmed by X-ray crystallographic analysis.

Red crystals of **2** were grown by vaporization of a CH_2Cl_2 solution at room temperature. The ORTEP plot of **2** is shown in Figure 3 and selected bond lengths and bond angles are collected in Table 2. Both of the rhenium atoms are in a distorted octahedral environment. The Re(2)–C(24) [1.966(3) Å] bond length is slightly longer than the Re(2)–C(25) distance [1.927(3) Å], which is an illustration of a stronger back-bonding interaction between Re(2) and C(25) (i.e. the pyridinyl nitrogen is a stronger donor than the arene carbon). The Re(2)–C(15) distance of 2.168(3) Å is within the normal range of Re–C bonds. Unlike complex **1**, the dihedral angles of N(1)–C(8)–C(9)–N(2) and C(15)–C(16)–C(17)–N(4) are 0.4(3)° and 4.1(4)°, respectively, which suggests that the naphthyridine core remains as a planar geometry.

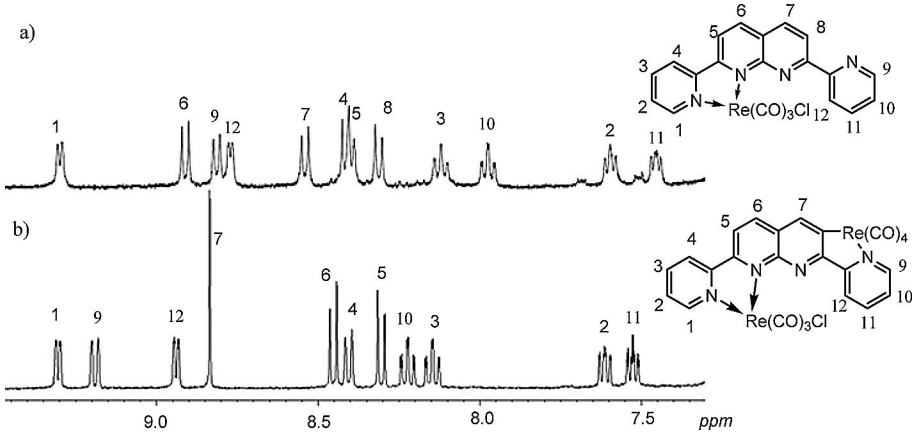

Figure 2. ^1H NMR spectra of (a) **1** and (b) **2** for the aromatic region.

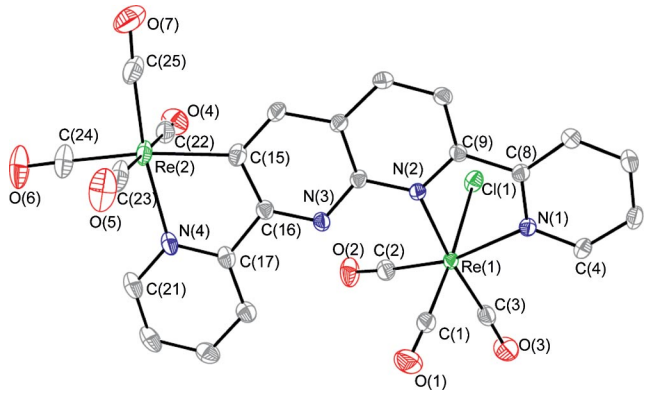

Figure 3. ORTEP plot of **2** (drawn with 30% probability ellipsoids).

Table 2. Selected bond lengths [Å] and angles [°] for **2**.

Bond length		Bond angles	
Re(1)–C(1)	1.908(3)	N(1)–Re(1)–N(2)	74.44(8)
Re(1)–C(2)	1.913(3)	N(1)–Re(1)–Cl(1)	79.84(6)
Re(1)–C(3)	1.914(3)	N(1)–Re(1)–C(1)	101.5(1)
Re(1)–N(1)	2.174(2)	N(1)–Re(1)–C(2)	166.3(1)
Re(1)–N(2)	2.181(2)	N(1)–Re(1)–C(3)	99.1(1)
Re(1)–Cl(1)	2.4777(7)	N(2)–Re(1)–C(3)	173.5(1)
Re(2)–C(22)	1.984(3)	N(4)–Re(2)–C(15)	76.5(1)
Re(2)–C(23)	2.005(4)	N(4)–Re(2)–C(22)	91.0(1)
Re(2)–C(24)	1.966(3)	N(4)–Re(2)–C(23)	89.3(1)
Re(2)–C(25)	1.927(3)	N(4)–Re(2)–C(24)	95.7(1)
Re(2)–C(15)	2.168(3)	N(4)–Re(2)–C(25)	171.2(1)
Re(2)–N(4)	2.199(2)	C(15)–Re(2)–C(24)	171.4(1)

Treatment of **2** with equal molar amount of $AgBF_4$ in CH_3CN readily provided the acetonitrile (ACN) coordinated complex, $[Re_2(bpnp)(CO)_7(ACN)]BF_4$ (**4**). Characterization of **4** was achieved by both spectroscopic and elemental analyses. The ESI-mass spectrum of **4** shows *m*/*z* = 894.15 and 853.15 for the ions of $[Re_2(bpnp)(CO)_7(ACN)]^+$ and $[Re_2(bpnp)(CO)_7]^+$, respectively. The ^1H NMR spectrum of **4** is similar to that of **2** except for the shift due to the methyl group of acetonitrile (δ = 2.15 ppm). Infrared carbonyl stretching frequencies appear at 2093, 2032, 1991, and 1920 cm^{-1}, which are quite similar to those of **2**.

Heterodinuclear Rhenium Complexes

Learning from the formation of **2** by means of *ortho*-metallation, we examined the possibility to prepare heterodinuclear rhenium complexes. Scheme 3 outlines the preparation of Re/Pd and Re/Ir complexes. Treatment of **1** with $[Ir(COD)Cl]_2$ followed by the silver salt yielded Re/Ir dinuclear complex **5**. Re/Pd complex **6** was obtained similarly by using Pd(COD)MeCl as the palladium ion source. Characterization of **5** and **6** was accomplished by NMR spectroscopic and mass spectroscopic analysis. The most informative proton nuclei, namely those that provide the most useful structural information, are those from the naphthyridine core (i.e. C5–C8 protons). These chemical shifts are summarized in Table 3. The disappearance of the shift at C8-proton in both **5** and **6** provides evidence that metallation occurred at that position. The downfield shifts (i.e. coordination chemical shifts) of H-9 protons for both **5** and **6** were also observed in these complexes, which supports the coordination of the pyridinyl nitrogen towards the metal centers. The coordination of acetonitriles in the complexes was verified by the methyl shifts of CH_3CN at δ = 2.05–2.30 ppm in the ^1H NMR spectra. The conductivities of **5** and **6** in acetonitrile were 109 and 167 $ohm^{-1}\,cm^2\,mol^{-1}$, indicative of the presence of a 1:1 and 2:1 electrolyte, respectively. The MALDI-mass spectrum of **5** shows *m*/*z* at 842.79, which corresponds to the formula of $C_{26}H_{20}N_7O_2IrRe$ [**5**-(CO)-(BF_4)]. Similarly, the peak at *m*/*z* = 787.73, which matches with the formula of $C_{23}H_{14}BF_4N_5O_3PdRe$ [**6**–**2**(CH_3CN) – BF_4], illustrates the dinuclear structure of **6**.

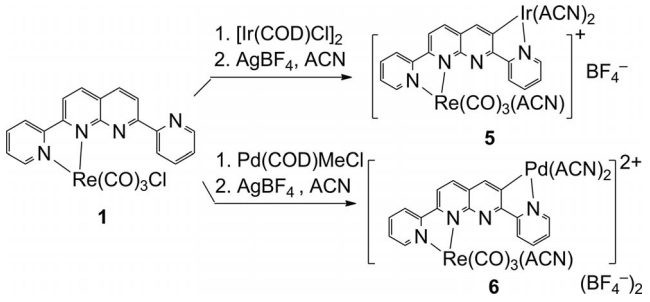

Scheme 3. Preparation of heterodinuclear complexes.

Table 3. ^1H NMR shifts of naphthyridine protons for **1**, **2**, **5**, and **6**.

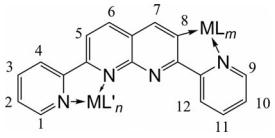

	H-5	H-6	H-7	H-8	H-9[a]
1	8.38 (d)	8.91 (d)	8.54 (d)	8.31 (d)	9.15 (d)
2	8.26 (d)	8.41 (d)	8.79 (s)		9.15 (d)
5	8.56 (d)	8.88 (d)	9.05 (s)		9.42 (d)
6	8.72 (d)	8.99 (d)	8.80 (s)		8.90 (d)

[a] The ^1H NMR shift of H-9 of free ligand bpnp is δ = 8.81 ppm.

Catalysis

It has been demonstrated that rhenium carbonyl complexes are active catalysts for the insertion of terminal acetylenes into β-keto esters, which subsequently undergoes cyclization to yield the pyranone derivatives (Scheme 4).[10] With these rhenium complexes in hand, their catalytic activities on the insertion of terminal acetylenes into β-keto

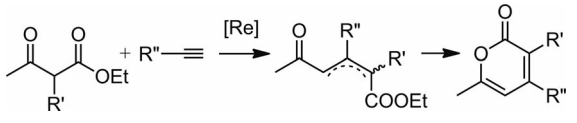

Scheme 4. Insertion of alkynes into β-keto esters followed by cyclization.

esters were investigated. In order to create an environmentally benign process, the catalytic reactions investigated in this work do not use any organic solvents.

We first examined the insertion of phenylacetylene into ethyl 2-methylacetoacetate catalyzed by **2** under photoirradiation at 350 nm. A series of screen tests suggested that carrying out the reaction of phenylacetylene (0.55 mmol), ethyl 2-methylacetoacetate (0.45 mmol), and **2** (0.5 mol-%) at 90 °C under irradiation at 350 nm for 12 h provides ethyl (2*E*)-2-methyl-5-oxo-3-phenyl-2-hexenoate (**7**) in 84% isolated yield [Equation (1)]. It is noted that photoirradiation is required in order to promote the reaction, presumably due to the photodissociation of carbonyl ligands that assist the coordination of substrates to the metal. Next, we ran a series of trial reactions based on Equation (1) in the presence of various rhenium complexes to compare the selectivity of these catalysts (Table 4). Based on the yield, all of the rhenium carbonyl complexes, except **10**, have activity in the insertion of phenylacetylene into acetoacetate to give **7** under the catalytic conditions described above. Among these catalysts, **2** and **4** prove to have the best activity in this insertion reaction, whereas other complexes show moderate activity.

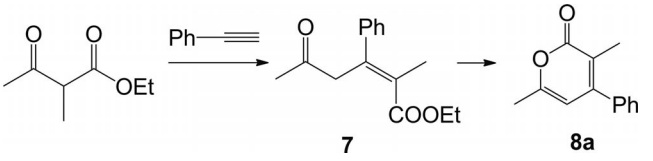

(1)

The cyclization of **7** to yield pyranone **8a** proceeded smoothly at 90 °C with tetrabutylammonium fluoride (TBAF) as the promoter. Thus, for the following study, we carried out the insertion reaction followed by the cyclization to provide the corresponding pyranone in a one-pot procedure. Table 5 summarizes the scope of the pyranone formation catalyzed by **2**. For example, the treatment of β-keto ester **Ia** with acetylene **IIb** in the presence of **2** (0.5 mol-%) at 90 °C under irradiation for 12 h, followed by the addition of TBAF (10 mol-%) and stirring the mixture at 90 °C for 12 h, gave 2-pyranone **8b** in 92% yield (Table 5, entry 2). Various terminal alkynes (**IIa**–**IIe**) react with 2-methylacetoacetate followed by cyclization to generate the corresponding pyranone (**8a**–**8e**) in excellent yields (Table 5, entries 1–5). Under similar reaction conditions, the reaction of 2-substituted acetoacetate with alkynes also provides good yields of the resulting products (Table 5, entries 6–8). These observations clearly demonstrate the excellent activity of **2** in the insertion of terminal acetylenes into β-keto esters. In terms of the catalytic activity, the turnover frequency (TOF) of **2** in the production of **8a** reaches 1.5 (mol·product)·(mol·catalyst)$^{-1}$·h^{-1}, which is superior to that of the known catalyst $[ReBr(CO)_3(THF)]_2$ (TOF: 0.23).[10]

Conclusions

In summary, we have reported the synthesis and characterization of a series of dinuclear complexes through *o*-me-

Table 4. Formation of **7** catalyzed by various rhenium complexes.[a]

Entry	Catalyst[b]		Yield
1	complex **1**	(0.5 mol-%)	53%
2	complex **2**	(0.5 mol-%)	84%
3	$Re_2(CO)_8(CH_3CN)_2$	(0.5 mol-%)	53%
4	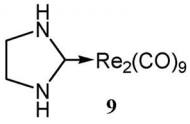 **9**	(1 mol-%)	31%
5	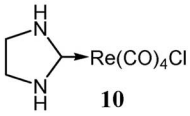 **10**	(1 mol-%)	22%
6	$Re(CO)_5Br$		69%
7	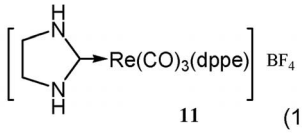 **11**	(1 mol-%)	trace
8	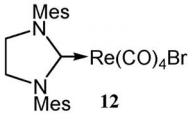 **12**	(1 mol-%)	28%
9	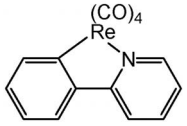 **13**	(1 mol-%)	16%
10	[(bipyridine)$Re(CO)_3Br$]	(1 mol-%)	53%
11	**4**	(0.5 mol-%)	80%
12	**5**		trace

[a] Reaction conditions: phenylacetylene (0.55 mmol), ethyl 2-methylacetoacetateate (0.45 mmol), and catalyst at 90 °C under irradiation at 350 nm for 12 h. [b] Mol-% based on the limiting reagent.

Table 5. Synthesis of 2-pyranones from β-keto esters and acetylenes.[a]

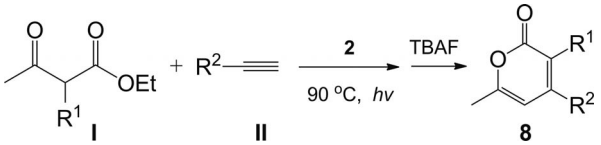

Entry	β-Keto ester	Acetylene	Yield[b] (%)
1	R^1 = Me **Ia**	R^2 = C_6H_5 **IIa**	**8a** (93)
2	R^1 = Me **Ia**	R^2 = *p*-MeC_6H_4 **IIb**	**8b** (92)
3	R^1 = Me **Ia**	R^2 = $C_6H_5CH_2$ **IIc**	**8c** (73)
4	R^1 = Me **Ia**	R^2 = $Cl(CH_2)_3$ **IId**	**8d** (87)
5	R^1 = Me **Ia**	R^2 = 1-cyclohexenyl **IIe**	**8e** (79)
6	R^1 = H **Ib**	R^2 = 1-cyclohexenyl **IIe**	**8f** (81)
7	R^1 = H **Ib**	R^2 = *p*-FC_6H_4 **IIf**	**8g** (51)
8	R^1 = $C_6H_5CH_2$ **Ic**	R^2 = C_6H_5 **Iia**	**8h** (90)

[a] Reaction conditions: acetylene (0.55 mmol), keto ester (0.45 mmol), and **2** (0.5 mol-%) at 90 °C under irradiation at 350 nm for 12 h. [b] Isolated yield.

tallation with the use of 2,7-dipyridinyl-1,8-naphthyridine (bpnp) as the ligand. The structures of these complexes were unambiguously determined by spectroscopic methods and through single-crystal X-ray analysis of **1** and **2**. Complex **2** appears to be catalytically active for the insertion of terminal acetylenes into ethyl 2-methylacetoacetates to give the substituted 5-oxo-2-hexenoates, which underwent cyclization to provide pyranones. Studies on the catalytic reactivity of these complexes are ongoing in our laboratory.

Experimental Section

General Information: All of the reactions and manipulation steps were performed under a nitrogen atmosphere. Dichloromethane and acetonitrile were dried with CaH_2 and distilled under nitrogen. The other chemicals and solvents were of analytical grade and were used after a degassing process. Ligand bpnp was prepared accordingly to the method reported previously.[8]

Nuclear magnetic resonance spectra were recorded in $CDCl_3$ or [D_6]acetone with a Bruker AVANCE 400 spectrometer. The chemical shifts are given in parts per million relative to Me_4Si for ^1H and ^{13}C NMR spectroscopy. The infrared spectra were measured with a Nicolet Magna-IR 550 spectrometer (Series-II). The UV/Vis spectra were recorded with a Hitachi U-2900 spectrometer.

Complex 1 and 2: A mixture of bpnp (20 mg, 0.07 mmol) and $Re_2(CO)_8(CH_3CN)_2$ (48 mg, 0.07 mmol) in chlorobenzene (2.5 mL) was sealed in a reaction tube. The mixture was heated at 200 °C for 4 h. After removal of the solvents, the residue was chromatographed on silica gel with 1% Et_3N/EtOAc as the eluent. A dark red band was collected to give **1** as a dark red solid (15.9 mg, 38%) and then a red band was collected to give **2** as a red solid (38.7 mg, 62%).

Complex 1: ^1H NMR (400 MHz, $CDCl_3$): δ = 7.45 (t, J = 5 Hz, 1 H, 11-H), 7.60 (t, J = 8 Hz, 1 H, 2-H), 7.96 (t, J = 8 Hz, 1 H, 10-H), 8.12 (t, J = 8 Hz, 1 H, 9-H), 8.31 (d, J = 8 Hz, 1 H, 8-H), 8.38 (d, J = 8 Hz, 1 H, 5-H), 8.40 (d, J = 8 Hz, 1 H, 4-H), 8.54 (d, J = 8 Hz, 1 H, 7-H), 8.72 (d, J = 5.2 Hz, 1 H, 12-H), 8.81 (d, J = 8 Hz, 1 H, 9-H), 8.91 (d, J = 8 Hz, 1 H, 6-H), 9.29 (d, J = 5.2 Hz, 1 H, 1-H) ppm. ^{13}C NMR (100 MHz, $CDCl_3$): δ = 119.7, 123.1, 123.2, 124.2, 1245.0, 127.0, 136.7, 137.7, 138.6, 140.3, 148.8, 153.1, 153.3, 153.8, 156.4, 159.3, 161.5, 189.7, 196.9, 197.7 ppm. IR (KBr): $\tilde{\nu}_{C=O}$ = 2015, 1908, 1884 cm^{-1}. FAB-HRMS: calcd. for $C_{21}H_{12}ClN_4O_3Re$ $[M]^+$ 590.0156; found 590.0153. $C_{21}H_{12}ClN_4O_3Re$ (590.00): calcd. C 42.75, H 2.05, N 9.50; found C 42.56, H 2.13, N 9.30.

Complex 2: ^1H NMR (400 MHz, $CDCl_3$): δ = 7.48 (t, J = 6.4 Hz, 1 H, 11-H), 7.56 (t, J = 6.4 Hz, 1 H, 2-H), 8.10 (t, J = 8 Hz, 1 H, 3-H), 8.17 (t, J = 8 Hz, 1 H, 10-H), 8.26 (d, J = 8.8 Hz, 1 H, 5-H), 8.36 (d, J = 8 Hz, 1 H, 4-H), 8.41 (d, J = 8 Hz, 1 H, 6-H), 8.79 (s, 1 H, 7-H), 8.89 (d, J = 5.2 Hz, 1 H, 12-H), 9.15 (d, J = 8 Hz, 1 H, 9-H), 9.26 (d, J = 5.2 Hz, 1 H, 1-H) ppm. ^{13}C NMR (100 MHz, $CDCl_3$): δ = 119.9, 124.6, 125.1, 126.8, 127.0, 127.3, 138.7, 138.8, 140.0, 150.3, 153.3, 153.7, 155.1, 157.5, 157.9, 161.3, 163.8, 171.2, 186.4, 187.2, 190.5, 191.1, 191.7, 197.9, 198.4 ppm. IR (KBr): $\tilde{\nu}_{C=O}$ = 2093, 2070, 1977, 1909 cm^{-1}. FAB-HRMS: calcd. for $C_{25}H_{11}ClN_4O_7Re_2$ $[M]^+$ 887.9432; found 887.9439. $C_{25}H_{11}ClN_4O_7Re_2$ (887.24): calcd. C 33.84, H 1.25, N 6.31; found C 33.67, H 1.35, N 6.01.

Complex 4: A mixture of **2** (15 mg, 0.017 mmol) and $AgBF_4$ (3 mg, 0.017 mmol) in anhydrous acetonitrile (2 mL) was heated at 90 °C for 5 h. The mixture was passed through celite to remove salts and the filtrate was concentrated to give **4** as a red powder solid (15 mg, 97%). ^1H NMR (400 MHz, $CDCl_3$): δ = 2.15 (s, 3 H, CH_3), 7.57 (t, J = 6.4 Hz, 1 H, 11-H), 7.74 (t, J = 6.4 Hz, 1 H, 2-H), 8.22 (t, J = 8 Hz, 1 H, 3-H), 8.39 (t, J = 8 Hz, 1 H, 10-H), 8.51 (d, J = 8 Hz, 1 H, 5-H), 8.62 (d, J = 8.8 Hz, 1 H, 4-H), 8.83 (d, J = 8 Hz, 1 H, 6-H), 8.90 (s, 1 H, 7-H), 8.97 (d, J = 5.2 Hz, 1 H, 12-H), 9.02 (d, J = 8 Hz, 1 H, 9-H), 9.16 (d, J = 5.2 Hz, 1 H, 1-H) ppm. ^{13}C NMR (100 MHz, $CDCl_3$): δ = 3.3, 121.4, 121.8, 125.0, 125.9, 126.7, 127.4, 128.1, 128.5, 139.7, 140.1, 140.8, 150.5, 152.7, 153.3, 155.2, 156.8, 158.3, 161.4, 162.8, 170.8, 186.5, 186.6, 190.5, 191.0, 193.7 ppm. IR (KBr): $\tilde{\nu}_{C=O}$ = 2093, 2032, 1991, 1920 cm^{-1}. ESI-HRMS: calcd. for $C_{27}H_{14}N_5O_7Re_2$ $[M - BF_4]^+$ 894.0008; found 894.0000. $C_{27}H_{14}BF_4N_5O_7Re_2$ (979.64): calcd. C 33.10, H 1.44, N 7.15; found C 32.87, H 1.38, N 6.82.

Complex 5: A mixture of **1** (10 mg, 0.017 mmol) and $[Ir(COD)Cl]_2$ (6 mg, 0.009 mmol) in CH_2Cl_2 was stirred at 40 °C for 12 h. The resulting red precipitate was collected and dissolved in CH_3CN. $AgBF_4$ (9.9 mg, 0.05 mmol) was added and the mixture was stirred at ambient temperature for 5 h. After removal of the solvent, the residue was precipitated in hexane/CH_3CN/CH_2Cl_2 to give **5** as a red solid (12 mg, 74%). ^1H NMR (400 MHz, $CDCl_3$): δ = 2.05 (br., 9 H, NC-CH_3), 7.71 (m, 1 H, 10-H), 7.81 (m, 1 H, 2-H), 8.21 (t, J = 7 Hz, 1 H, 11-H), 8.36 (t, J = 7.6 Hz, 1 H, 3-H), 8.56 (d, J = 8.8 Hz, 1 H, 5-H), 8.71 (d, J = 8.8 Hz, 1 H, 4-H), 8.88 (d, J = 8 Hz, 6-H), 8.93 (d, J = 8 Hz, 12-H), 9.05 (s, 1 H, 7-H), 9.21 (br., 1 H, 1-H), 9.42 (t, J = 7.6 Hz, 1 H, 9-H) ppm. ^{13}C NMR (100 MHz, $CDCl_3$): δ = 3.7, 3.8, 121.82, 126.63, 126.74, 128.73, 129.1, 139.8, 141.1, 141.6, 142.7, 143.0, 151.3, 152.2, 152.8, 155.1, 158.1, 158.5, 160.2, 169.4, 192.1, 195.1, 196.2 ppm. IR (KBr): $\tilde{\nu}_{C=O}$ = 2018, 1903, 1892 cm^{-1}. MALDI-MS: calcd. for $C_{26}H_{20}N_7O_2IrRe$ [M – (CO) – $(BF_4)]^+$ 894.0008; found 842.19. $C_{27}H_{20}BF_4IrN_7O_3Re$ (955.72): calcd. C 33.93, H 2.11, N 10.26; found C 33.57, H 1.96, N 9.89.

Complex 6: The procedure was similar to that for complex **5**. (9 mg, 68%). ^1H NMR (400 MHz, $CDCl_3$): δ = 2.32 (br., 9 H, NC-CH_3), 7.63 (t, J = 6 Hz, 1 H, 10-H), 7.86 (t, J = 6.4 Hz, 1 H, 2-H), 8.09 (t, J = 8 Hz, 1 H, 11-H), 8.42 (t, J = 8 Hz, 1 H, 3-H), 8.53 (d, J = 8 Hz, 1 H, 12-H), 8.72 (d, J = 8 Hz, 1 H, 5-H), 8.80 (s, 1 H, 7-H), 8.77 (d, J = 7 Hz, 1 H, 4-H), 8.90 (d, J = 7 Hz, 1 H, 9-H), 8.99 (d, J = 5 Hz, 1 H, 6-H), 9.26 (d, J = 5 Hz, 1 H, 1-H) ppm. ^{13}C NMR (100 MHz, $CDCl_3$): δ = 2.7, 122.3, 123.7, 124.8, 125.6, 125.8, 126.7, 127.8, 130.1, 138.7, 140.7,141.9, 143.9, 151.1, 155.1, 155.2, 155.7, 157.9, 161.8, 163.3, 192.1, 195.5,195.7 ppm. IR (KBr): $\tilde{\nu}_{C=O}$ = 2035, 1934 (br) cm^{-1}. FAB-HRMS: calcd. for $C_{23}H_{14}BF_4N_5O_3PdRe$ [M – 2·(CH_3CN) – BF_4] 787.9718; found 787.9723. $C_{27}H_{20}B_2F_8N_7O_3PdRe{\cdot}CH_3CN$: calcd. C 34.91, H 2.32, N 11.23; found C 34.48, H 2.03, N 10.87.

Crystallography: Crystals suitable for X-ray determination were obtained for **1**·(H_2O) and **2** by recrystallization at room temperature. Cell parameters were determined with a Siemens SMART CCD diffractometer. The structure was solved by using the SHELXS-97 program[11] and refined by using the SHELXL-97 program[12] by full-matrix least-squares on $F2$ values. CCDC-909557 (for complex **2**), -909558 (for complex **1**) contain the supplementary crystallographic data for this paper. These data can be obtained free of charge from The Cambridge Crystallographic Data Centre via www.ccdc.cam.ac.uk/data_request/cif.

Complex 1·(H_2O): $C_{21}H_{14}ClN_4O_4Re$, triclinic, space group $P\bar{1}$, a = 9.94520(10) Å, b = 10.41760(10) Å, c = 10.41760(10) Å; α = 77.7510(10)°, β = 73.5270(10)°, γ = 64.9680(10)°, V = 1007.454(17) $Å^3$, Z = 2, $\rho_{calcd.}$ = 2.004 mgm^{-3}, $F(000)$ 584, crystal size = 0.20 × 0.15 × 0.10 mm^3, reflections collected 23387; indepen-

dent reflections 4617 [R(int) = 0.0290]; θ range 3.03 to 27.50°; goodness-of-fit on $F2$ 1.032; final R indices [$I > 2\sigma(I)$]: $R1$ = 0.0158, $wR2$ = 0.0415; R indices (all data): $R1$ = 0.0175, $wR2$ = 0.0425.

Complex 2: $C_{25}H_{11}ClN_4O_7Re_2$, monoclinic, space group $C2/c$, a = 29.8108(3) Å, b = 12.69290(10) Å, c = 13.6408(2) Å, α = 90°, β = 96.5190(10)°, γ = 90°, V = 5128.11(10) Å^3, Z = 8, $\rho_{calcd.}$ = 2.298 mgm^{-3}, F(000) 3296, crystal size = 0.25 × 0.20 × 0.15 mm^3, reflections collected 30424, independent reflections 5878 [R(int) = 0.0252], θ range 3.01 to 27.50°, goodness-of-fit on $F2$ 1.011, final R indices [$I > 2\sigma(I)$]: $R1$ = 0.0160, $wR2$ = 0.0401, R indices (all data): $R1$ = 0.0183, $wR2$ = 0.0412.

Catalysis: The typical procedure for the insertion of an alkyne into ethyl 2-methylacetoacetate followed by cyclization is as follows: a mixture of alkyne (0.55 mmol), keto ester (0.45 mmol), and rhenium complex **2** (2.3 × 10^{-3} mmol) was heated at 90 °C under irradiation at 350 nm for 12 h. Tetrabutylammonium fluoride (0.045 mmol) was then added and heated at 90 °C for another 10 h. After completion of the reaction, brine (3 mL) and CH_2Cl_2 (5 mL) were added. The organic layer was separated and the aqueous layer was extracted with CH_2Cl_2. The combined organic extracts were dried with magnesium sulfate and concentrated. The products were purified by chromatography with elution of CH_2Cl_2/EtOAc and characterized by ^{1}H and ^{13}C NMR spectroscopy. Complexes **9** to **12** were prepared according to the reported method.[13]

3,6-Dimethyl-4-phenyl-2*H*-pyran-2-one (8a):[10] ^{1}H NMR (400 MHz, $CDCl_3$): δ = 2.05 (s, 3 H), 2.28 (s, 3 H), 2.16 (s, 3 H),5.98 (s, 1 H), 7.26–7.30 (m, 2 H), 7.40–7.45 (m, 3 H) ppm. ^{13}C NMR (100 MHz, $CDCl_3$): δ = 13.77, 19.58, 106.59, 118.15, 127.87, 128.56, 128.74, 137.80, 152.04, 157.79, 164.84 ppm.

3,6-Dimethyl-4-*p*-tolyl-2*H*-pyran-2-one (8b): ^{1}H NMR (400 MHz, $CDCl_3$): δ = 2.05 (s, 3 H), 2.25 (s, 3 H), 2.40 (s, 3 H), 5.97 (s, 1 H), 7.19 (d, J = 7.2 Hz, 2 H), 7.25 (d, J = 7.2 Hz, 2 H) ppm. ^{13}C NMR (100 MHz, $CDCl_3$): δ = 13.82, 19.56, 21.27, 106.69, 117.84, 127.88, 129.21, 134.84, 138.81, 152.10, 157.64, 164.91 ppm. IR (KBr): $\tilde{\nu}_{CO}$ = 1710 cm^{-1}. ESI-HRMS: calcd. for $C_{14}H_{15}O_2$ [M + H] 215.107; found 215.1068.

4-Benzyl-3,6-dimethyl-2*H*-pyran-2-one (8c): ^{1}H NMR (400 MHz, $CDCl_3$): δ = 2.11 (s, 3 H), 2.13 (s, 3 H), 3.74 (s, 2 H), 5.71 (s, 1 H), 7.11 (d, J = 8 Hz, 2 H), 7.22–7.32 (m, 3 H) ppm. ^{13}C NMR (100 MHz, $CDCl_3$): δ = 19.56, 38.53, 106.10, 106.13, 118.29, 126.71, 128.48, 128.65, 139.97, 151.58, 157.66, 164.32 ppm. IR (KBr): $\tilde{\nu}_{CO}$ = 1720 cm^{-1}. ESI-HRMS: calcd. for $C_{14}H_{15}O_2$ [M + H] 215.1072; found 215.1079.

4-(3-Chloropropyl)-3,6-dimethyl-2*H*-pyran-2-one (8d): ^{1}H NMR (400 MHz, $CDCl_3$): δ = 1.97–2.04 (m, 2 H), 2.07 (s, 3 H), 2.21 (s, 3 H), 2.59 (t, J = 7.6 Hz, 2 H), 3.57 (t, J = 6.4 Hz, 2 H), 5.84 (s, 1 H) ppm. ^{13}C NMR (100 MHz, $CDCl_3$): δ = 11.95, 19.52, 29.93, 31.09, 43.95, 105.92, 118.41, 152.04, 158.04, 164.41 ppm. IR (KBr): $\tilde{\nu}_{CO}$ = 1719 cm^{-1}. ESI-HRMS: calcd. for $C_{10}H_{14}O_2Cl$ [M + H] 201.0682; found 201.0679.

4-Cyclohexenyl-3,6-dimethyl-2*H*-pyran-2-one (8e):[10] ^{1}H NMR (400 MHz, $CDCl_3$): δ = 1.63–1.70 (m, 2 H), 1.70–1.77 (m, 2 H), 2.01 (s, 3 H), 2.03–2.13 (m, 2 H), 2.13–2.18 (m, 2 H), 2.19 (s, 3 H), 5.65 (t, J = 8 Hz, 1 H), 5.80 (s, 1 H) ppm. ^{13}C NMR (100 MHz, $CDCl_3$): δ = 13.43, 19.47, 21.77, 22.49, 25.01, 27.68, 105.32, 116.79, 128.03, 135.31, 154.95, 157.58, 165.12 ppm.

4-Cyclohexenyl-6-methyl-2*H*-pyran-2-one (8f): ^{1}H NMR(400 MHz, $CDCl_3$): δ = 1.62–1.68 (m, 2 H), 1.70 (s, 3 H), 1.73–1.80 (m, 2 H), 2.23–2.32 (m, 7 H), 6.04 (s, 1 H), 6.15 (s, 1 H), 6.47 (t, J = 8 Hz, 1 H) ppm. ^{13}C NMR (100 MHz, $CDCl_3$): δ = 20.03, 21.56, 22.31, 25.47, 26.22, 101.14, 105.46, 132.80, 132.98, 155.39, 160.19, 164.29 ppm. IR (KBr): $\tilde{\nu}_{CO}$ = 1719 cm^{-1}. ESI-HRMS: calcd. for $C_{12}H_{15}O_2$ [M + H] 191.1072; found 191.1064.

4-(4-Fluorophenyl)-6-methyl-2*H*-pyran-2-one (8g): ^{1}H NMR (400 MHz, $CDCl_3$): δ = 2.34 (s, 3 H), 6.28 (s, 1 H), 6.32 (s, 1 H), 7.16–7.20 (m, 2 H), 7.56–7.60 (m, 2 H) ppm. ^{13}C NMR (100 MHz, $CDCl_3$): δ = 20.19, 103.25, 107.96, 116.20, 116.42, 128.63, 128.71, 131.92, 154.35, 162.33, 162.96, 163.24 ppm. IR (KBr): $\tilde{\nu}_{CO}$ = 1713 cm^{-1}. ESI-HRMS: calcd. for $C_{12}H_{10}O_2F$ [M + H] 205.0665; found 205.0664.

3-Benzyl-6-methyl-4-phenyl-2*H*-pyran-2-one (8h): ^{1}H NMR (400 MHz, $CDCl_3$): δ = 2.28 (s, 3 H), 3.84 (s, 2 H), 6.02 (s, 1 H), 7.09 (d, J = 7.4 Hz, 2 H), 7.16–7.20 (m, 2 H), 7.20–7.28 (m, 5 H), 7.42–7.44 (m, 3 H) ppm. ^{13}C NMR (100 MHz, $CDCl_3$): δ = 19.70, 32.91, 106.88, 120.89, 126.07, 127.58, 128.26, 128.32, 128.68, 128.88, 137.70, 139.72, 153.70, 158.93, 164.19 ppm. IR (KBr): $\tilde{\nu}_{CO}$ = 1714 cm^{-1}. ESI-HRMS: calcd. for $C_{19}H_{17}O_2$ [M + H] 277.1229; found 277.1223.

Acknowledgments

We thank the National Science Council, Taiwan for financial support (grant number NSC-100-2113-M002-001-MY3).

[1] a) D. C. Powers, T. Ritter, *Acc. Chem. Res.* **2012**, *45*, 840–850; b) R. D. Adams, B. Captain, *Acc. Chem. Res.* **2009**, *42*, 409–418; c) M. H. Perez-Temprano, J. A. Casares, P. Espinet, *Chem. Eur. J.* **2012**, *18*, 1864–1884; d) M. Shibasaki, S. Matsunaga, N. Kumagai, *Synlett* **2008**, 1583–1602; e) S. Maggini, *Coord. Chem. Rev.* **2009**, *253*, 1793–1832.
[2] P. Caluwe, *Macromolecules* **1979**, *12*, 803–808.
[3] a) W. R. Tikkanen, E. Binamira-Soriaga, W. C. Kaska, P. C. Ford, *Inorg. Chem.* **1984**, *23*, 141–146; b) W. R. Tikkanen, E. Binamira-Soriaga, W. C. Kaska, P. C. Ford, *Inorg. Chem.* **1983**, *22*, 1147–1148.
[4] E. Binamira-Soriaga, N. L. Keder, W. C. Kaska, *Inorg. Chem.* **1990**, *29*, 3167–3171.
[5] a) W. R. Tikkanen, C. Krueger, K. D. Bomben, W. L. Jolly, W. C. Kaska, P. C. Ford, *Inorg. Chem.* **1984**, *23*, 3633–3638; b) B.-S. Liao, Y.-H. Liu, S.-M. Peng, S.-T. Liu, *Dalton Trans.* **2012**, *41*, 1158–1164.
[6] F.-M. Yang, P.-Y. Chen, C.-C. Lee, Y.-H. Liu, S.-M. Peng, S.-T. Liu, *Dalton Trans.* **2012**, *41*, 5782–5784.
[7] W. Tikkanen, W. C. Kaska, S. Moya, T. Layman, R. Kane, C. Krueger, *Inorg. Chim. Acta* **1983**, *76*, L29–L30.
[8] G. R. Newkome, S. J. Garbis, V. K. Majestic, F. R. Fronczek, G. Chiari, *J. Org. Chem.* **1981**, *46*, 833–839.
[9] P. Kurz, B. Probst, B. Spingler, R. Alberto, *Eur. J. Inorg. Chem.* **2006**, 2966–2974.
[10] Y. Kuninobu, A. Kawata, M. Nishi, H. Takata, K. Takai, *Chem. Commun.* **2008**, 6360–6362.
[11] *SHELXS-90*: G. M. Sheldrick, *Acta Crystallogr., Sect. A* **1990**, *46*, 467–473.
[12] G. M. Sheldrick, *SHELXL-97*, University of Göttingen, Germany, **1997**.
[13] C.-H. Chen, Y.-H. Liu, S.-M. Peng, J.-T. Chen, S.-T. Liu, *Dalton Trans.* **2012**, *41*, 2747–2754.

Received: November 22, 2012
Published Online: March 1, 2013

